Macromolecules
ARTICLE

Macromolecules **2009**, *42*, 5053–5061 **5053**
DOI: 10.1021/ma900751y

Synthesis and Helical Conformation of Novel Optically Active Liquid Crystalline Poly(*p*-phenylene)s Containing Cyanoterphenyl Mesogen as Pendant

Lie Chen,[†] Yiwang Chen,*[,†] Kai Yao,[†] Weihua Zhou,[†] Fan Li,[†] Liping Chen,[‡] Rongrong Hu,[§] and Ben Zhong Tang[§]

[†]*Institute of Polymers/Department of Chemistry, Nanchang University, Xuefu Road 999, Nanchang 330031, China,* [‡]*Department of Chemical Engineering, East China Jiaotong University, Nanchang 330013, China, and* [§]*Department of Chemistry, The Hong Kong University of Science & Technology (HKUST), Clear Water Bay, Kowloon, Hong Kong*

Received April 7, 2009; Revised Manuscript Received May 5, 2009

ABSTRACT: Novel liquid crystalline poly(*p*-phenylene)s (PPP) bearing cyanoterphenyl mesogenic pendants with varying spacer lengths {$-[C_6H_3-COO-terphenyl-CN]_n-$, **P(0)**; $-[C_6H_3-COO-(CH_2)_6-O-terphenyl-CN]_n-$, **P(6)**} were designed and synthesized, and the effects of structural variations on the liquid crystallinity behaviors and the optical properties of the polymers are studied. **P(0)** shows an SmA phase with faint birefringence, while **P(6)** readily forms the enantiotropic SmA_d phase with a colorful fan texture, due to the longer flexible spacer favoring the better packing arrangements. Photoexcitation of their solutions induces strong blue light emission. The photoluminescence of **P(6)** in THF solution is much stronger and red-shifted to the visible spectral region, even extending to 600 nm, than that of **P(0)**. The longer spacer may have better segregated the bulky chromophoric pendants, which effectively hampers the excitons from traveling to the quenching sites of the backbone and hence enhances the stronger emission in the photoluminescence. No significant shifts in the emission maxima are observed when the polymers are fabricated into thin films, suggesting that the segregation of the backbone effectively decreases the strong interchain interaction. Another interesting and outstanding property also could be found in this type of polymers. Due to the stric crowding, cyanoterphenyl mesogen pendants orientating around the main chain forces the main chain showing spiral conformation along the main chain in the long region; moreover, a short spacer is favorable.

Introduction

Conjugated polymers with liquid crystalline (LC) groups in their side chains are attracting current interests, because they afford anisotropies in electrical and optical properties when they are macroscopically aligned.[1,2] In this type of LC conjugated polymer, the main chain can be aligned by virtue of spontaneous orientation of the LC side chain. Besides, macroscopic alignment of LC domains is achieved by an external force such as shear stress, electric or magnetic field.[3] The control of the orientation of conjugated polymer main chains gives rise to the possibility of polarized electroluminescent devices.[4] A variety of side-chain liquid-crystalline conjugated polymers (SCLCCP) were endowed with such properties as mesomorphism, luminescence, photoconductivity, gas permeability, and chain helicity by introducing various founctional groups onto the conjugated skeleton.[5−20]

Poly (*p*-phenylene) (PPP) is a typical conjugated polymer with excellent mechanical properties and thermal and thermooxidative stability. Besides, poly(*p*-phenylene)s are good blue light emitting polymers, which be particularly interesting because strong blue emitters are still rare and blue light can act as "color converters" to meet the need of a full-color display.[21] However, PPP becomes insoluble, infusible, and intractable at more than six repeat units. This has been a serious problem that has prevented elucidation of the relationship between the polymer chain structure and properties and has limited its applications.[22] Compared to the instability and intractability of PPP, substituted PPP shows thermal stability, good solubility, excellent luminescence, and photoconductivity by introducing different mesogens such as light-emitting chromophores and chiral groups. Chen et al.[23] have synthesized a class of thermotropic nematic and chiral-nematic conjugated poly(*p*-phenylene) carrying cyanobiphenyl light-emitting chromophores and (−)-cholesterol (showing as following structure) as pendant groups, which were attested to produce significant degrees of linearly and circularly polarized photoluminescence by alignment. Akagi[24] recently synthesized a group of ferroelectric liquid crystalline polyphenylene derivatives, through substitution of fluorine-containing chiral LC groups into side chains (showing as following structure), the polymers exhibited a quick response to electric field.

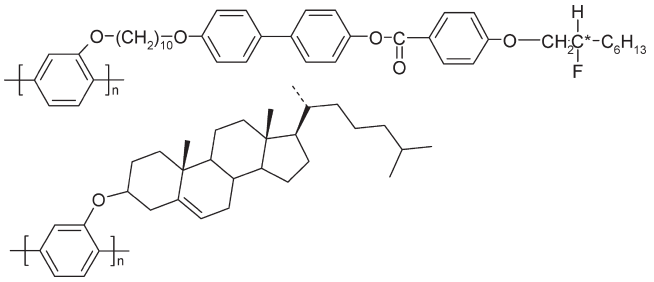

In our previous study, we synthesized a group of polyacetylenes containing cyanoterphenyl mesogenic pendants and found that

*Corresponding author. Telephone: +86 791 3969562. Fax: +86 791 3969561. E-mail: ywchen@ncu.edu.cn.

Published on Web 05/22/2009

the cyanoterphenyl mesogen pendants endowed the polymer with good mesomorphism and high luminescence, besides, the energy could be transferred from mesogen to main chain to favor the fluorescence efficiency.[25,26] This encouraged us to extend our investigations to design other liquid crystalline conjugated polymers (LCCPs) based on different backbone containing cyanoterphenyl mesogenic pendants and check how the structural variations exert their effect on the properties. The terphenyl is not only a chromophore but also a mesogenic core. Thus, if one is combining optically active terphenyl with electronically active PPP at the molecular level, the spontaneous orientation and chromophoric property of the terphenyl mesogens might likely lead to materials with novel, outstanding, and interesting properties. The terphenyl mesogen groups as a pendant linked to the backbone might transfer its energy to the backbone and provide polymers with high light-emitting. For this reason, our group has attempted to design and synthesize poly(*p*-phenylene)s containing cyanoterphenyl mesogen with a short ester bridge spacer. In order to check the influence of the spacer length on structures and properties of polymers, its cousin polymer with longer flexible spacer has also been prepared. The effects of structural variations on the liquid crystallinity behaviors and the optical properties of the polymers are studied. Besides, due to the stric crowding, cyanoterphenyl mesogen pendants orientating around the main chain induces the main chain to exhibit helical conformation in the long region. Therefore, the secondary structures of polymers have also been given special attention.

Experimental Section

Materials. Trimethyl borate, *n*-butyllithium, 2,5-dibromotoluene, 6-bromo-1-hexanol, trimethyl borate, 4-(4-bromophenyl) phenol, 4-bromobenzonitrile, $NiCl_2$, 1,3-dicyclohexylcarbodiimine (DCC), 4-(dimethylamino)pyridine (DMAP), and tetrakis(triphenylphosphine)palladium were purchased from Alfa Aesar and used as received without any further purification. Tetrahydrofuran (THF) was dried over sodium. Other chemicals were obtained from Shanghai Reagent Co., Ltd., and used as received.

Techniques. The nuclear magnetic resonance (NMR) spectra were collected on a Bruker ARX 400 NMR spectrometer with deuterated chloroform or THF or DMSO as the solvent and with tetramethylsilane ($\delta = 0$) as the internal standard. The infrared (IR) spectra were recorded on a Shimadzu IRPrestige-21 Fourier transform infrared (FTIR) spectrophotometer by drop-casting sample solution on KBr substrates. The ultraviolet−visible (UV) spectra of the samples were recorded on a Hitachi UV-2300 spectrophotometer. The fluorescence measurement for photoluminescence (PL) of the polymers was carried out on a Shimadzu RF-5301 PC spectrofluorophotometer with a xenon lamp as the light source. The gel permeation chromatography (GPC), so-called size-exclusion chromatography (SEC) analysis, was conducted with a Breeze Waters system equipped with a Rheodyne injector, a 1515 Isocratic pump and a Waters 2414 differential refractometer using polystyrenes as the standard and tetrahydrofuran (THF) as the eluent at a flow rate of 1.0 mL/min and 40 °C through a Styragel column set, Styragel HT3 and HT4 (19 mm × 300 mm, $10^3 + 10^4$ Å) to separate molecular weight (MW) ranging from 10^2 to 10^6. Thermogravimetric analysis (TGA) was performed on a PerkinElmer TGA 7 for thermogravimetry at a heating rate of 20 °C/min under nitrogen with a sample size of 8−10 mg. Differential scanning calorimetry (DSC) was used to determine phase-transition temperatures on a Perkin-Elmer DSC 7 differential scanning calorimeter with a constant heating/cooling rate of 10 °C/min. Texture observations by polarizing optical microscopy (POM) were made with a Nikon E600POL polarizing optical microscope equipped with an Instec HS 400 heating and cooling stage. The X-ray diffraction (XRD) study of the samples was carried out on a Bruker D8 Focus X-ray diffractometer operating at 30 kV and 20 mA with a copper target ($\lambda = 1.54$ Å) and at a scanning rate of 1°/min. Circular dichroism (CD) is recorded on a JASCO J-810 spectropolarimeter. Elemental analyses (EA) were characterized by means of elemental analysis with Vario Elementar III. The mass spectra were recorded on a Finnigan TSQ 7000 triple quadrupole mass spectrometer operating in a chemical ionization (CI) mode using methane as carrier gas.

Scheme 1. Illustration of Procedures for Synthesis of P(0) and P(6)

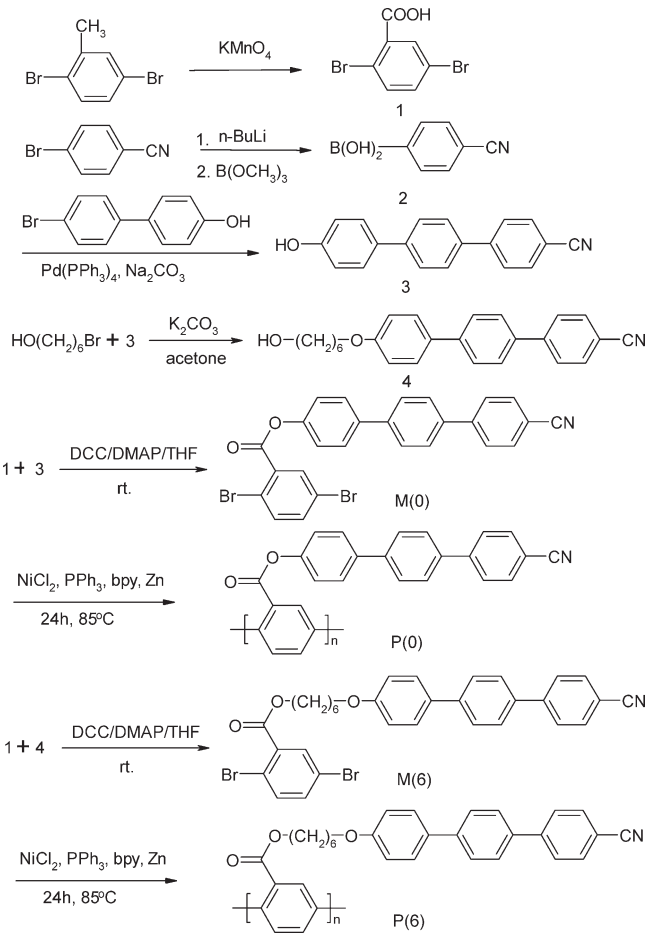

Synthesis of the Monomers. The synthesis and structures of the monomers are outlined in Scheme 1. All the reactions and manipulations were carried out under a nitrogen atmosphere.

2,5-Dibromobenzoic Acid. 2,5-Dibromotoluene, 8.0 g (32.0 mmol), and 20 g of $KMnO_4$ were dissolved in 150 mL of pyridine and 250 mL of water; the mixture was heated at reflux for 2 h. Then 40 g of $KMnO_4$ was added several times and the reaction kept refluxing overnight. The MnO_2 precipitate was filtered and washed with boiling water. The filtrate was concentrated and the product was precipitated by addition of HCl. The acid product was dried overnight at 80 °C in a vacuum oven. 86% yield. IR (KBr, cm^{-1}): 3030 (Ar−H), 2822 (broad, −OH), 1709 (C=O), 1577, 1471, 1399, 1115, 1087, 575, 487.

4-Cyanobenzeneboronic Acid. A solution of *n*-butyllithium (30 mL, 2.87 M in hexane, 0.086 mol) was added dropwise to a stirred, cooled (−110 °C) solution of 4-bromobenzonitrile (15 g, 0.082 mol) in dry THF (180 mL) under dry nitrogen. The solution was stirred at below −100 °C for 1 h and a solution of trimethyl borate, 20.8 mL in dry THF (60 mL), was added at below −100 °C. The solution was allowed to warm to room temperature overnight. The 10% hydrochloric acid was added and the solution was stirred for 1 h at room temperature. The product was extracted into ether and the organic layer

was washed with water and dried with $MgSO_4$.The solvent was removed *in vacuo* and the crude product dissolved in THF and precipitated with n-hexane to give a yellow solid with yield of 70%.

4-Hydroxy-4′-cyanoterphenyl. Under a dry nitrogen atmosphere a solution of 2.00 g of 4-cyanobenzeneboronic acid (13.6 mmol) in 10 mL of ethanol was added to a solution of 2.75 g of 4-(4′-bromophenyl)phenol (97%, 11.02 mmol) and 0.42 g of tetrakis(triphenylphosphine)palladium(0) (99%, 0.36 mmol) in 20 mL of benzene and 20 mL of aqueous Na_2CO_3 (2 M). The reaction was conducted under reflux overnight. The reaction mixture was then shaken with ethyl acetate and the insoluble parts were filtered off. The organic layer was dried with anhydrous $MgSO_4$, and the solvent was removed by evaporation *in vacuo*. The crude product was recrystallized from acetone to provide a yellow powder, 65% yield. IR (KBr, cm^{-1}): 2215 (C≡N), 3351 (−OH). ^{1}H NMR (ppm, $CDCl_3$): 7.73−7.65 (m, aromatic, 8H), 7.53 (d, aromatic, 2H), 6.93 (d, aromatic, 2H ortho to hydroxyl), 4.91 (s, 1H, −OH).

4-(6-Hydroxyhexyloxy)-4′-cyanoterphenyl. After 20 mmol of 4-hydroxy-4′-cyanoterphenyl, 24 mmol of 6-bromo-1-hexanol, 40 mmol of K_2CO_3, and 4.01 mmol of KI were mixed together in 200 mL of DMF, the reaction mixture was refluxed at 80 °C for 24 h. It was then cooled and the solvent was removed by evaporation *in vacuo*. The residue was recrystallized from absolute ethanol to give a light yellow solid in 73% yield. IR (KBr, cm^{-1}): 3416, 3033, 2935, 2852, 2228, 1600, 1491, 1258, 1047, 812. ^{1}H NMR (ppm,THF-*d*): 7.64−7.77 (m, aromatic, 8H), 7.58−7.62 (d, aromatic,2H), 6.87−6.89 (d, aromatic, 2H), 4.55 (t, 1H, −OH), 3.89−3.92 (t, 2H, $-CH_2OAr-$), 3.36−3.39 (t, $-CH_2O$ OC, 2H),1.33−1.72 (m, 8H, $-(CH_2)_4$).

2,5-Bromo-1-[(4-(4′-cyano)terphenyloxy)carbonyl]benzene M (0). 2,5-Dibromobenzoic acid (3.36 g, 12 mmol) was added to a mixture of 4-hydroxy-4′-cyanoterphenyl (2.71 g, 10 mmol), (dimethylamino)pyridine, DMAP 1.47 g (12 mmol), and dicyclohexylcarbodiimide, DCC (2.46 g, 12 mmol), in 30 mL of absolute THF and further stirred for 24 h at room temperature under an argon atmosphere. Then the solution was filtered to remove the urea crystals, and the solvent was removed by evaporation. The crude product was purified by column chromatography (*n*-hexane/$CHCl_3$ = 1/4) to afford **M(0)** as white powder. Yield: 72%. IR (KBr, cm^{-1}): 2228, 1713, 1602, 1491, 804, 501. ^{1}H NMR (ppm, $CDCl_3$): 8.17 (s, aromatic, 1H), 7.76−7.69 (m, aromatic, 10H), 7.63, 7.61 (d, aromatic, 1H), 7.56, 7.55 (d, aromatic, 1H), 7.37−7.35(d, aromatic, 2H ortho to −O−). MS (CI): *m*/*e* 533.3 [(M^+), calcd 533]. Anal. Calcd for $C_{26}H_{15}O_2NBr_2$: C, 58.54; H, 2.81. Found: C, 59.02; H, 2.94.

2,5-Bromo-1-[(6-(4-(4′-cyano)terphenyloxy)hexyloxy)carbonyl]-benzene M(6). 2,5-Dibromobenzoic acid (3.36 g, 12 mmol) was added to a mixture of 4-(6-hydroxyhexyloxy)-4′-cyanoterphenyl (3.71 g, 10 mmol), (dimethylamino)pyridine (DMAP, 1.47 g, 12 mmol), and dicyclohexylcarbodiimide (DCC, 2.46 g, 12 mmol), in 200 mL of absolute THF and further stirred for 24 h at room temperature under an argon atmosphere. Then the solution was filtered to remove the urea crystals, and the solvent was removed by evaporation. The crude product was purified by column chromatography (*n*-hexane/$CHCl_3$ = 1/4) to afford **M(6)** as white powder. Yield = 70%. IR (KBr, cm^{-1}): 2935, 2863, 2218, 1705, 1604, 1491, 816, 495. ^{1}H NMR (ppm, $CDCl_3$): 7.90 (s, aromatic, 1H), 7.75−7.66 (m, aromatic, 10H), 7.58, 7.56(d, aromatic, 1H), 7.46, 7.45(d, aromatic, 1H), 7.00−6.98(d, aromatic, 2H ortho to −O−), 4.38−4.35 (t, 2H, $-CH_2-O-Ar$), 4.04−4.01 (t, 2H, $-CH_2-OOC-$), 1.85−1.25 (m, 8H, $-CH_2(CH_2)_4CH_2-$). MS (CI): *m*/*e* 633.2 [(M^+), calcd 633]. Anal. Calcd for $C_{32}H_{27}O_3NBr_2$: C, 60.66; H, 4.27. Found: C, 60.85; H, 4.35.

Polymerization. All the polymerization reactions and manipulations were carried out under nitrogen using Schlenk techniques in a vacuum line system or in an inert-atmosphere glovebox (Vacuum Atmospheres), except for the purification of the polymers, which was done in an open atmosphere. A typical experimental procedure for the polymerization of **P(0)** is given below.

A 50 mL three necks round-bottom flask equipped with condenser, rubber septum, nitrogen inlet−outlet and magnetic stirrer was charged under nitrogen with 0.533 g (1.0 mmol) of **M(0)**, 0.08 g (0.0304 mmol) of PPh_3, 2.024 g (30.96 mmol) of Zn, 0.0076 g (0.05 mmol) of bpy, 0.0064 g (0.05 mmol) of $NiCl_2$ and 5 mL of dry dimethyl acetamide (DMAC). The reaction was performed at 85 °C, under nitrogen. The mixture was stirred for 24 h. Then, the polymer was precipitated into excess methanol/HCl mixture, filtered, and dried. The polymer was then redissolved in THF and precipitated in methanol. A gray solid was obtained.

P(0), gray solid: IR (KBr, cm^{-1}): 2228, 1733, 1602, 1491, 806. ^{1}H NMR (ppm, DMSO-d_6): 8.21 (s, aromatic, 1H), 7.96−7.38 (m, aromatic, 14H). M_n = 19842; M_w/M_n = 1.16. UV (THF, 0.05 mM), $\lambda_{max}/\varepsilon_{max}$: 317 nm/3.55 × 10^4 mol^{-1} L cm^{-1}.

P(6), gray solid: IR (KBr, cm^{-1}): 2933, 2854, 2218, 1713, 1592, 1481, 806. ^{1}H NMR (ppm, THF-*d*): 8.00−7.90 (m, aromatic, 1H), 7.79−7.47 (m, aromatic, 12H), 6.88−6.86(d, aromatic, 2H ortho to −O−), 4.30−4.25 (t, 2H, $-CH_2-O-Ar$), 3.92−3.91 (t, 2H, $-CH_2-OOC-$), 1.71−1.18 (m, 8H, $-CH_2(CH_2)_4-CH_2-$). M_n = 21979; M_w/M_n = 1.74. UV (THF, 0.05 mM), $\lambda_{max}/\varepsilon_{max}$: 315 nm/3.51 × 10^4 mol^{-1} L cm^{-1}.

Results and Discussion

Synthesis of the Monomers. The 4-hydroxy-4′-cyanoterphenyl was synthesized through a Suzuki reaction between 4-cyanobenzeneboronic acid and 4-(4′-bromophenyl)phenol using tetrakis(triphenylphosphine)palladium(0) as the catalyst. In order to introducing the longer spacer, 4-(6-hydroxyhexyloxy)-4′-cyanoterphenyl was prepared by 4-hydroxy-4′-cyanoterphenyl and 6-bromo-1-hexanol via etherification. Finally, two poly(*p*-phenylene)s monomers were prepared by esterifications of 2,5-dibromo benzoic acid with 4-(6-hydroxyhexyloxy)-4′-cyanoterphenyl and 4-(6-hydroxyhexyloxy)-4′-cyanoterphenyl, respectively, in the presence of 1,3-dicyclohexylcarbodiimine (DCC), *p*-toluenesulfonic acid (TsOH), and 4-(dimethylamino)pyridine (DMAP). The reactions went smoothly, and the products were isolated in high yields (≥70%) after purifications by silica gel chromatography followed by recrystallization. The structures of all the intermediates and the final monomers were confirmed by FT-IR, ^{1}H NMR, MS, and EA. (see the Experimental Section for details).

Synthesis of the Polymers. Regioregularity plays an important role in properties of conjugated polymers. Many functionalized regioregular conjugated polymers show fascinating properties such as high conductivity, mobility, chemosensitivity, liquid crystallinity, or chirality.[27,28] A number of synthetic routes for producing poly(*p*-phenylene)s have been described in the literature, and current methodologies for the direct synthesis of derivatized poly(*p*-phenylene)s are primarily based upon nickel-complex polycondensation (Yamamoto reaction) and palladium-mediated cross-coupling reactions (Suzuki coupling) due largely to their preservation of regiochemistry and nearly quantitative yields.[29] The Yamamoto reaction can tolerate the functional groups and offers polymers with high regioregularity and good solubility. Thus, in order to produce regioregular poly(*p*-phenylene)s with excellent properties, the polymerizations were carried out via the Yamamoto reaction with Ni-complex catalysts. All polymers synthesized were fusible and soluble in common organic solvents including THF, DMAC, and DMF, etc. The chemical structures of the polymers were confirmed by FT-IR, ^{1}H NMR, and EA.

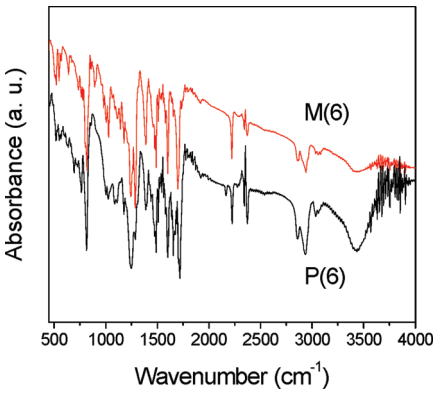

Figure 1. FT-IR spectra of the monomer **M(6)** and polymer **P(6)**.

Structural Characterization. All the purified polymerization products gave satisfactory spectroscopic data corresponding to their expected molecular structures (see Experimental Section for details). A typical example of the IR spectrum of **P(6)** is shown in Figure 1. The spectrum of its monomer **M(6)** is also shown in the same figure for comparison. The monomers absorbs at 2218, 1705, 495 cm^{-1}, due respectively to the C≡N stretching, the C═O stretching and the C−Br bending vibrations. The C−Br bending vibrations (~500 cm^{-1}) for the monomers almost disappeared in the spectra of their corresponding polymers, indicating that the monomers have been completely transformed to the polymers via dehalogenative polycondensation with the Ni-based complex catalysts. Figure 2 shows the ^{1}H NMR spectra of the isolated polymers in comparison with that of monomers, which sufficiently supports the structure of the products by the assignments of the signals as described in the Experimental Section . The resonance peaks in the ^{1}H NMR spectra of polymers are broader than that of monomers, indicating that the monomers had been polymerized successfully. The sharp signal at about 8.25 ppm in the spectra of **P(0)** is assigned to the protons of phenylene rings of the repeat unit in head-to-tail diad, whereas the weak signal at about 8.40 ppm is attributed to other types of linkages (head-to-head or tail-to-tail), indicating that the polymer possesses high regioregularity. The signal of the protons of head-to-tail diad in **P(6)** also can be observed at near 8.00 ppm. Except the peaks of solvent and water remained in the spectra, no unexpected signals are observed in the spectra of the monomers and polymers, and all the resonance peaks can be assigned to appropriate protons as marked in Figure 2. The EA and MS described in the Experimental Section further confirmed the structures of the products.

Thermal Stability. Since the formation of mesophases of thermotropic liquid crystals are realized by the application of heat, the thermal stability of the polymers is thus of primary concern. Polymer **P(0)** and **P(6)** are thermally stable and lose almost no weight at a temperature as high as ~350 °C in the thermogravimetric analysis. The thermal stability of the polymers is further substantiated by the DSC analysis: no irreversible peaks suspiciously associated with polymer degradation are observed at the high temperatures during the cycles of repeated heating−cooling scans. The cyanoterphenyl mesogenic appendages may have well wrapped the conjugated backbones and thus protect them from the perturbations by heat and attacks by the degradative species.

Mesomorphic Properties. After confirming the thermal stability of the polymers, we investigated the monomers' and polymers' mesomorphic properties. Figure 3 shows microphotographs of the mesomorphic textures of **M(0)**, **M(6)** and their polymeric products **P(0)**, **P(6)**, taken under a polarized optical microscope (POM). Both of the monomers exhibit enantiotropic optical anisotropy with focal conic fan texture or batonnet-like structure when heated or cooled; this suggests that the mesophasic nature of **M(0)** and **M(6)** are smectic phases and the mesomorphism is enantiotropic. Generally, if the mesogenic pendant is closely "coupled" with

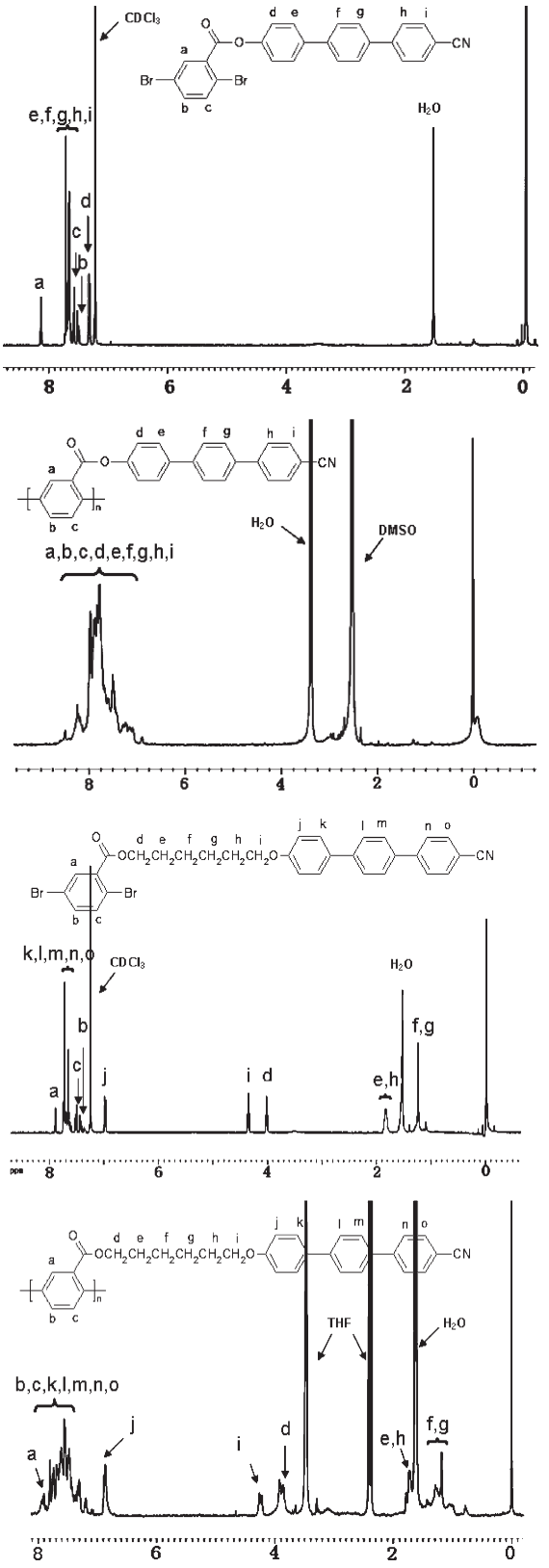

Figure 2. ^{1}H NMR spectra of monomers and polymers.

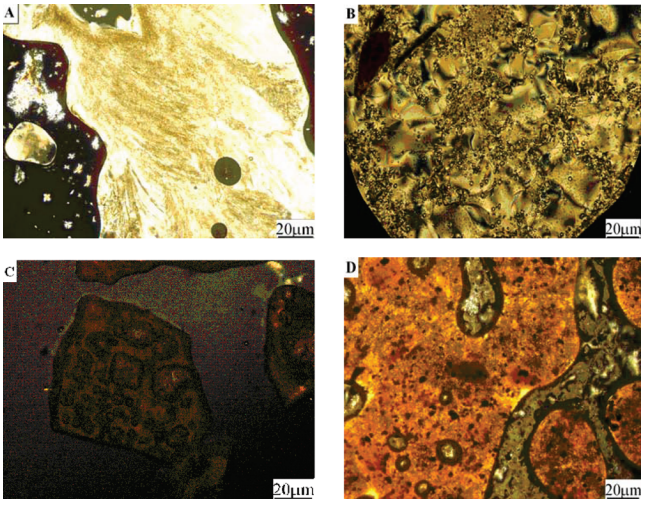

Figure 3. Mesomorphic textures observed on cooling (A) **M(0)** to 145 °C, (B) **M(6)** to 120 °C, (C)**P(0)** to 273 °C, and (D) **P(6)** to 210 °C from their isotropic melts.

the rigid backbone, it will destroy the packing arrangements of the mesogens and demolish the stability of the mesophases. Previous studies[25,30] on the mesomorphic properties of the type of LCCP with rigid backbone and short spacers, such as {−[HC═C(CH_2O−terph−CN)]−}, have revealed that the short spacers and bulkly mesogen pendants rendered the polymers completely nonmesomorphic, although their corresponding monomers were liquid crystalline and exhibit order packing. So the case also may also be occurred in **P(0)** because of the short ester linkage and bulk cyanoterphenyl group. To our surprise, when **P(0)** is cooled from its isotropic state, small optically anisotropic entities actually emerge from the dark background of the isotropic liquid, although the exact nature of the mesophase is difficult to identify and the fine textures cannot grow to large monodomains. It has been reported that the carbonyloxy bridge allows better ordering.[31] That is, on one hand, the bulk mesogen partially distorts the packing arrangements of the mesogens and impedes the growth of the liquid crystalline domains, on the other hand, the ester group also affects the mesophase formation and favors the better packing arrangements. The competition between the constructive and destructive effects may have led to the faint birefringence. Reheating **P(0)** also can generate the birefringent texture. With the aid of X-ray diffraction (XRD) measurement, the textures are identified to be associated with a mixture of SmA phase (vide post). When the −$(CH_2)_6$O− is inserted between the rigid backbone and mesogen and the spacer length is increased, delightfully, the anisotropic entities of **P(6)** is growing the bigger colorful texture and developing better than that of **P(0)**. The SmA_d phase readily form, thanks to the flexibility of the longer spacer, which allows the mesogen to move together to pack in a regular fashion.

To learn more about the thermal transitions of the monomers and polymers, we measured their thermograms under nitrogen on a differential scanning calorimeter. Figure 4 shows the DSC thermograms of the monomers and polymers. When **M(0)** is allowed to cool from the isotropic state to 148.7 °C, fan texture of the SmA phase is observed and the monomer completely solidifies at 141.5 °C under POM. The exothermic peaks at the lower temperature may thus be associated with crystal transformation from one state to another (k−k transition).[32] In the second heating cycle of **M(0)**, its corresponding k−SmA and SmA−i transitions are detected at 174.6 and 187.3 °C. The mesomorphism is thus

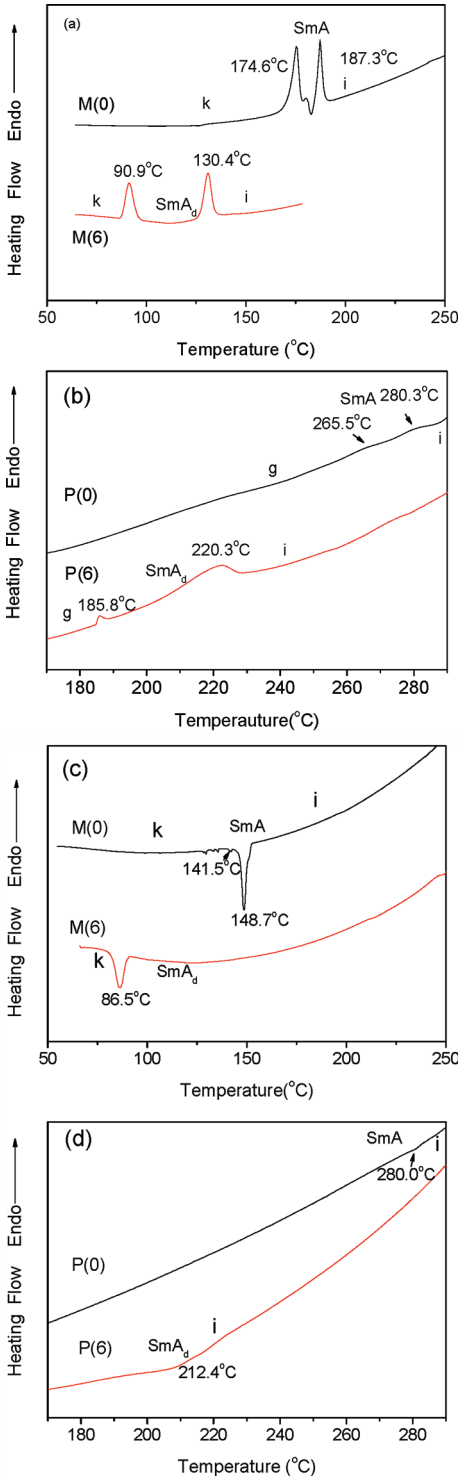

Figure 4. DSC thermograms of the monomers and polymers recorded under nitrogen during (a and b) the second heating, and (c and d) first cooling scans at a scan rate of 10 °C/min.

enantiotropic. On heating of **M(6)** at a rate of 10 °C/min^{-1}, it enters the SmA_d mesophase from its solid state at 90.9 °C. The mesophase is stable in a temperature range over 39.5 °C before **M(6)** finally melts into its isotropic state at 130.4 °C. In the first cooling scan of **M(6)**, in agreement with the observation by POM, a SmA_d−k transition is detected at 86.5 °C. Its corresponding i−SmA_d transition is not shown in the cooling scan, probably due to the fast cooling rate, but can be notarized at 122.1 °C by POM. The melting temperature of **M(6)** is lower than that of **M(0)**, owning to the

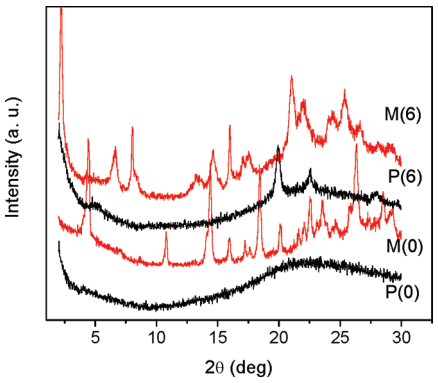

Figure 5. X-ray diffraction patterns of the monomers and polymers quenched from their liquid crystalline states.

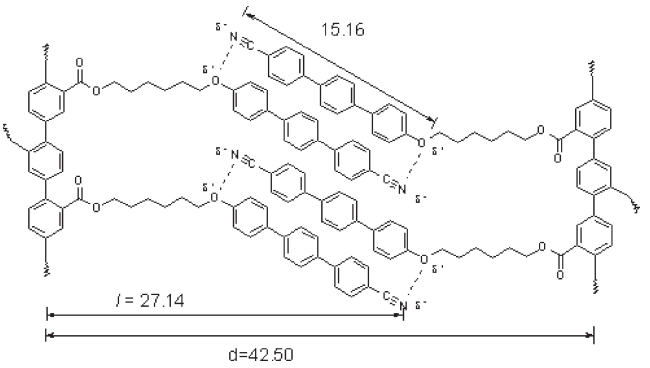

Figure 6. Proposed bilayer packing arrangement of **P(6)** within the SmA_d layer with the smectogens interdigitating in antiparallel fashion.

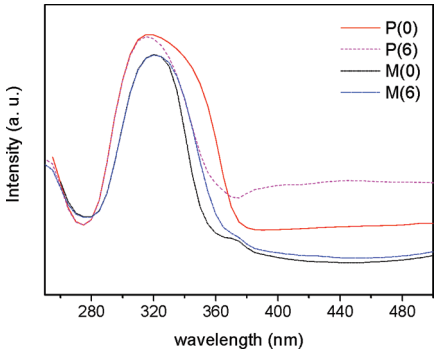

Figure 7. UV spectra of THF solutions of the monomers and the mesogenic poly(*p*-phenylene)s (0.05 mM).

plasticization effect of the longer flexible spacers. In the second heating cycle of **P(0)**, weak endothermic peaks associated with its g−SmA transition and SmA−i transition are observed at 265.5 and 280.3 °C, respectively, and the corresponding i−SmA transition is detected at 280.0 °C in the first cooling scan. When the spacer length is increased in **P(6),** the mesophasic transition peaks become sharper and readily detectable in both cooling and heating scan. Clearly, the longer spacer offers more freedom for the polymer segments and the mesogenic pendants to act separately.[32] Its g−SmA_d transition and SmA_d−i transition are shown at 185.8 and 220.3 °C; moreover, a broad exothermic peak associated with the i−SmA_d transition is exhibited at 212.4 °C, which often can be observed in SCLCCP.[26,32]

XRD analysis can provide useful information concerning molecular arrangement, mode of packing, and type of order in a mesophase of a polymeric liquid crystal. The XRD patterns were obtained from the mesogenic poly(*p*-phenylene)s and their monomers quenched with liquid nitrogen from liquid-crystalline states, whereas the mesophases in the liquid-crystalline states were frozen by the rapid quenching with liquid nitrogen. **M(0)** shows several Bragg reflections at high angles, and also displays a sharp reflection at a low-angle of $2\theta = 4.43°$ (shown in Figure 5) corresponding to a layer spacing of 19.93 Å, which is almost as to the calculated molecular length of **M(0)** in its most extended conformation (l = 19.45 Å), thus providing a smectic A mesophase in a monolayer arrangement. The XRD diffractogram of **M(6)** also displays Bragg reflections at low and high angles. The sharp reflection at the low angle ($2\theta = 2.2°$) corresponds to a layer spacing of 40.08 Å, which is longer than the molecular length (28.40 Å). Because the d/l ratio is ∼1.40, the bilayer structure is thus an SmA_d type, in which the cyanoterphenyl mesogen are interdigitated in an antiparallel fashion. In agreement with the POM and DSC, **P(6)** exhibits smectic phase with good packing arrangement. **P(6)** shows not only the peak in the high angle region, but also Bragg reflections at middle and low angles. The peak located at $2\theta = 20.0°$ (d = 4.44 Å) is corresponded to the interside chain distance, that is, the distance between the mesogenic core of the side chains. The sharp reflection at $2\theta = 2.05°$ corresponded to a layer spacing of 42.50 Å, which is considerably in excess of the molecular length of the repeat unit of **P(6)** in its most extended conformation (l = 27.14 Å).The mesophase of the polymer thus may consist of such a bilayer structure as schematically shown in Figure 6, in which the mesogens arrange in an antiparallel overlapping interdigitated manner, giving a d/l ratio of ∼1.50, a value often found in the SmA_d mesophase. The near-neighbor pairing of the partially negatively charged cyano group with the partially positively charged phenoxy group actually further supporting the proposed bilayer packing arrangement of the polymer molecules within the SmA layer.[31] In the midangle region, the diffractogram of the polymer **P(6)** shows a weak reflection at $2\theta = 5.09°$, from which a d-spacing of 16.67 Å. The calculated length for the interdigitated (cyanoterphenylyl)oxy groups in the proposed bilayer structure of **P(6)** is 15.1 Å. The reflection peak at $2\theta = 5.09°$ thus may be related to the regions, in which the rigid (cyanoterphenylyl)oxy groups are interdigitated and well packed. In contrast to the **P(6)**, the XRD diffractogram of the **P(0)** shows more diffuse and exhibits less reflection peaks. This suggests that the bulk and rigid side chain and the short spacer decrease the packing arrangement in the polymer. The broad hump peaked at $2\theta = 20.8°$, from which a d-spacing of 4.26 Å is derived from Bragg's law. The sharp reflection at the low angle (2θ = 2.04°) corresponds to a layer spacing of 42.10 Å, which is in considerable is close to the double of molecular length of the repeat unit (18.30 Å). This confirms the SmA nature of the mesophase and suggests that the mesogens are packed in a bilayer structure.

Electronic Absorption and Photoluminescence. The absorption spectra of the tetrahydrofuran (THF) solutions of the monomers and polymers are given in Figure 7. The UV spectra of **M(0)** and **M(6)** are detected as strong absorption at 322 nm, associated with the K-band of the cyanoterphenyl mesogen. Polymers of **P(0)** and **P(6)** absorb strongly at 317 and 315 nm, respectively, assignable to the $\pi-\pi^*$ bands of the cyanoterphenyl mesogenic pendant, because the monomers and polymers have similar absorption wavelengths. None of the monomers shows any peaks at wavelengths longer than 375 nm, while the UV spectra of the polymers well extend to beyond 500 nm. The absorption in the long-wavelength visible spectral region is thus obviously from the poly(*p*-phenylene) backbone of the polymers. The intensity

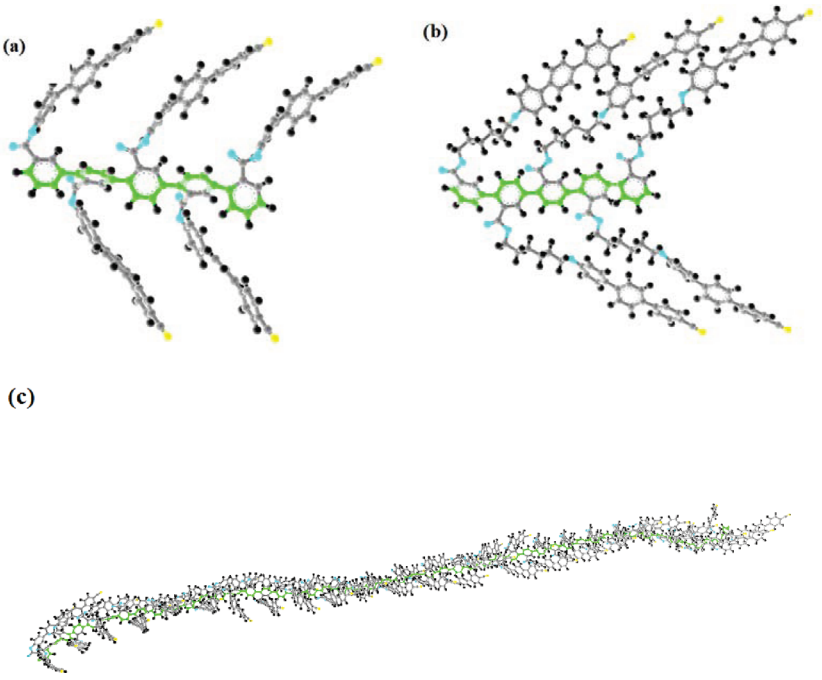

Figure 8. Computer-generated representation of (a) **P(0)** with five repeat unts, (b) **P(6)** with five repeat units, and (c) spiral direction of **P(0)** with fifty repeat unts.

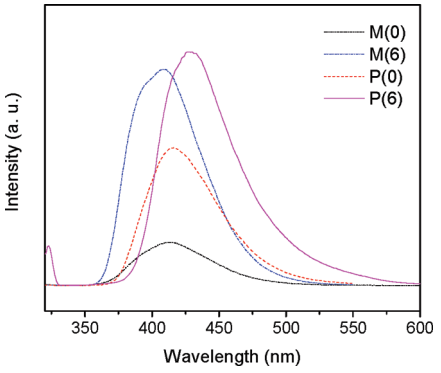

Figure 9. Photoluminescence spectra of the monomers and polymers in THF solutions (0.05 mM). Excitation wavelength: 320 nm.

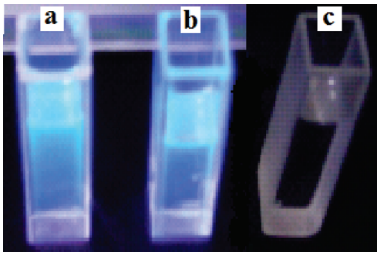

Figure 10. Photographs of blue fluorescence of the polymers in THF solution: (a) **P(6)**, (b) **P(0)**, and (c) pure THF, excited by irradiation of UV light of 320 nm.

of **P(6)** in the long-wavelength region is much stronger than that of **P(0)**, This is in agreement with our previous observations that the longer spacer reduces steric crowding and allows the backbone to be more coplanar than the short spacer, thus resulting in the observed hyperchromic effect.[25] Computer-generated molecular geometry of **P(6)** shows a better coplanarity than that of **P(0)** in Figure 8.

A polymer with both liquid-crystalline and light emitting properties may find unique technological applications. We thus investigated the fluorescence properties of the polymers in dilute THF solutions (Figure 9). Upon photoexcitation at 320 nm, the peak maxima of **M(0)** and **M(6)** are located at 412 and 408 nm, respectively, however, light emitting bands of their corresponding polymers are shifted to the longer regions with the higher intensity. It suggests that the emitting center is both the mesogenic cyanoterphenyl pendant and the backbone, and energy transfer from the cyanoterphenyl pendant to the backbone favors the stronger light-emitting of backbone. The PL of **P(6)** is much stronger than that of **P(0)**, and red-shifted to the visible spectral region, even extending to 600 nm. The quantum efficiency (Φ_F) of the **P(0)** and **P(6)** are 42% and 51% respectively. The increase of emission intensity and quantum efficiency with the spacer length in this case is associated with the studies by us and others, because the longer spacer may have better segregated the bulkly chromophoric pendants, which effectively hampers the excitons from traveling to the quenching sites of the backbone and hence enhances the stronger emission in the photoluminescence. The photo graphs of bule flurescence of the polymers in THF solution, excited by irradiation of UV light of 320 nm, are shown in Figure 10, and pure THF is also shown in the same figure for comparison.

Most conjugated polymers emit intensely in solution but become weak emitters when fabricated into films.[33,34] This is mainly caused by strong interchain interaction. In the solid state, the polymer strands aggregate together to form less luminescent species such as excimers, leading to red-shifted emissions with low efficiencies. We thus fabricated the polymers into film to check their fluorescence properties. Delightfully, both of the polymers remain their strong light emitting properties, and no significant shifts in the peak maximum are observed in comparison to those in the solutions. This is suggestive of little excimer absorption and emission, and the segregation of the backbone effectively decreases the strong interchain interaction. The comparison between PL of the solid state and solution state is shown in Figure 11.

Secondary Structure of the Polymers. Synthetic helical polymers with π-conjugation along the main chains is under

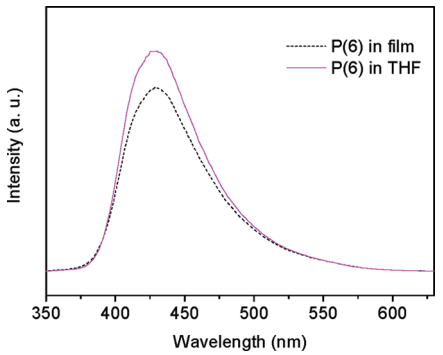

Figure 11. Photoluminescence spectra of **P(6)** in THF solutions (0.05 mM) and in the film state. Excitation wavelength: 320 nm.

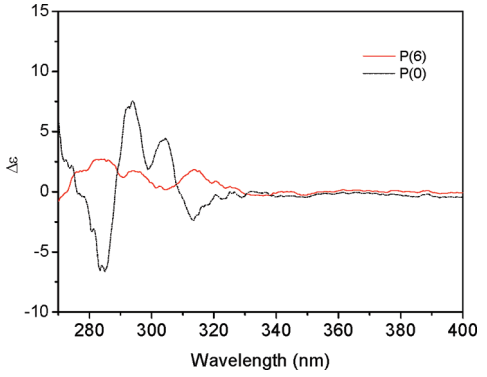

Figure 12. CD spectra of **P(0)** and **P(6)** measured in THF ($c = 0.25$ mM).

hot pursuit in recent years due to the challenge they offer in polymer chemistry as well as their wide practical and potential applications, such as optical polarizing films, chiral stationary phases, asymmetric electrodes, nisotropic molecular wires, fluorescent chemosensors.[35] Generally, helical conjugated polymers are obtained by the introduction of chiral substituents, polymerization using a chiral catalystic system, or preparation in a chiral liquid crystalline solvent, a new method reported by Goto and his coworkers.[36] Increasing the bulkiness of the chiral pendants can enhance the persistence length of the helix and thus increase the Cotton effects.[37]

We have a great interest in checking how the bulkly and heavy mesogenic pendants exert their influence on the secondary structure of the polymers. The "jacked effect" from the bulkly and heavy cyanoterphenyl mesogen orientating around the backbone and the repellent from stric crowding between the pendants, especially in **P(0)**, probably result in the spiral direction of the poly(*p*-phenylene)s in the long region. We thus conducted CD spectroscopic analysis of the polymers to confirm the assumption. Figure 12 depicts the CD spectra of **P(0)** and **P(6)** measured in THF. Although there have no any chiral groups/center in the structures of the polymers, **P(0)** shows strong Cotton effects at 284, 294, 305, and 315 nm, while **P(6)** exhibits strong Cotton effects at 284, 293, and 313 nm, which are located in the UV absorption region, unambiguously proving that these polymers adopt a helical conformation with a preferred screw sense, which originates from the backbone. Polymer **P(0)** exhibits even stronger Cotton effects than those of **P(6)**, probably due to the steric effect of bulky liquid-crystalline mesogens and a direct connection with the main chain preventing the planar conformation of the poly(*p*-phenylene) backbone, consequently, leading to the obvious helical conformation of the main chain. Computer-generated molecular geometry of **P(0)** further confirms the spiral direction of the main chain. By comparing **P(0)** with **P(6)**, we can conclude that due to the steric crowding, cyanoterphenyl mesogen pendants orientating around the main chain forces the main chain to show a spiral conformation along the main chain in the long region, and the short spacer enhances the tendency.

Conclusion

In this work, we designed and synthesized a group of poly(*p*-phenylene) monomers and polymer, and introduce the chromophoric cyanoterphenyl mesogenic pendant at the centrobaric position onto the poly(*p*-phenylene) main chain with different spacer length. The effects of the structural variations on the chemical and physical properties of the monomers and polymer were investigated. The Ni-based complex is a effective catalyst for poly(*p*-phenylene) monomers with functional groups to produce polymer with stereoregular structure. Thanks to the cyanoterphenyl mesogen pendants, the polymers possess high heat stabilities. The spacer length exerts great influence on the liquid crystallinity and the optical properties of the polymers. The monomers and polymers are all liquid crystalline and exhibit enantiotropic mesophases when heated or cooled. **M(0)** shows an SmA mesophase, whereas **M(6)** shows SmA_d mesophases. **P(0)** shows SmA phase bilayer arrangement with faint mosegenic texture, due to the steric crowding inhibiting the better packing. **P(6)**, compared with the polymer with short spacer length **P(0)**, readily forms the SmA_d phase with colorful birefringent texture. **P(0)** and **P(6)** show strong electronic absorption and high photoluminescence. Their solution can emit strong blue light and the longer spacer hences enabling light emission. The polymers thin films also luminescences intensely at the wavelengths similar to those in the solutions, indicating that the polymers remain emissive in the aggregation station.

Another important conclusion mentioned here is that, in order to reduce the repellent from stric crowding, the cyanoterphenyl mesogen pendant orientating around the skeleton can force the main chain to be helical conformation in the long region and the short spacer will enhance the tendency. Cheerfully, it has opened a new charming pathway to create novel LCCP containing the helical main chain without introducing any chiral center. On the other hand, the short spacer always pay destructive effects on the mesomorphic properties, thus, how to balance the advantages and disadvantages to find out the effects of the structural variables on helical screw and how to optimize the structures of the polymers to obtain excellent novel optically active material is our orientation.

Acknowledgment. Financial support for this work was provided by the National Natural Science Foundation of China (50773029), the Natural Science Foundation of Jiangxi Province (2007GZC1727 and 2008GQH0046), Jiangxi Provincial Department of Education, the Program for New Century Excellent Talents in University (NCET-06-0574), and Program for Innovative Research Team of Nanchang University, Program for Innovative Research Team in University of Jiangxi Province, and Program for Changjiang Scholars and Innovative Research Team in University (IRT0730).

References and Notes

(1) Oh, S.-Y.; Akagi, K.; Shirakawa, H.; Araya, K. *Macromolecules* **1993**, *26*, 6203.
(2) Akagi, K.; Shirakawa, H. In *Electrical and Optical Polymer Systems: Fundamentals, Methods, and Applications*; Wise, D. L., Wnek, G. E., Trantolo, D. J., Cooper, T. M., Gresser, J. D., Eds.; Marcel Dekker: New York, 1998; Vol 28, pp 983−1010.
(3) Osaka, I.; Goto, H.; Itoh, K.; Akagi, K. *Synth. Met.* **2001**, *119*, 541.
(4) Goto, H.; Dai, X.; Ueoka, T.; Akagi, K. *Macromolecules* **2004**, *37*, 4783.

(5) Yuan, W. Z.; Sun, J. Z.; Dong, Y.; Haeussler, M.; Yang, F.; Xu, H. P.; Qin, A.; Lam, J. W. Y; Zheng, Q.; Tang, B. Z. *Macromolecules* **2006**, *39*, 8011.
(6) Okoshi, K.; Sakajiri, K.; Kumaki, J.; Yashima, E. *Macromolecules* **2005**, *38*, 4061.
(7) Akagi, K.; Guo, S.; Mori, T.; Goh, M.; Piao, G.; Kyotani, M. *J. Am. Chem. Soc.* **2005**, *127*, 14647.
(8) Xing, C.; Lam, J. W. Y.; Zhao, K.; Tang, B. Z. *J. Polym. Sci., Part A: Polym. Chem.* **2008**, *46*, 2960.
(9) Zhou, J.-L.; Chen, X.-F.; Fan, X.-H.; Chai, C.-P.; Lu, C.-X.; Zhao, X.-D.; Pan, Q.-W.; Tang, H.-Y.; Gao, L.-C.; Zhou, Q.-F. *J. Polym. Sci., Part A: Polym. Chem.* **2006**, *44*, 4532.
(10) Sanda, F.; Araki, H.; Masuda, T. *Macromolecules* **2004**, *37*, 8510.
(11) Lai, L. M.; Lam, J. W. Y.; Qin, A.; Dong, Y.; Tang, B. Z. *J. Phys. Chem. B* **2006**, *110*, 11128.
(12) Li, B. S.; Kang, S. Z.; Cheuk, K. K. L. L.; Wan, L.; Ling, L.; Bai, C.; Tang, B. Z. *Langmuir* **2004**, *20*, 7598.
(13) Yuan, W. Z.; Mao, Y.; Zhao, H.; Sun, J. Z.; Xu, H. P.; Jin, J. K.; Zheng, Q.; Tang, B. Z. *Macromolecules* **2008**, *41*, 701.
(14) Yuan, W. Z.; Qin, A.; Lam, J. W. Y.; Sun, J. Z.; Dong, Y.; Haeussler, M.; Liu, J.; Xu, H. P.; Zheng, Q.; Tang, B. Z. *Macromolecules* **2007**, *40*, 3159.
(15) Cheuk, K. K. L.; Liu, J.; Xe, Z.; Xu, K.; Tang, B. Z. *Macromolecules* **2002**, *35*, 1229.
(16) Dong, Y.; Lam, J. W. Y.; Han, P.; Cheuk, K. K. L.; Kwok, H. S.; Tang, B. Z. *Macromolecules* **2004**, *37*, 6408.
(17) Lam, J. W. Y.; Dong, Y.; Kwok, H. S.; Tang, B. Z. *Macromolecules* **2006**, *39*, 6997.
(18) Percec, V.; Asandei, A. D.; Hill, D. H.; Crawford, D. *Macromolecules* **1999**, *32*, 2597.
(19) Soto, J. P.; Diaz, F. R.; Valle, M. A.; Nunez, C. M.; Bernede, J. C. *Eur. Polym. J.* **2006**, *42*, 935.
(20) Zhao, X.; Hu, X.; Zheng, P. J.; Gan, L. H.; Lee, C. K. P. *Thin Solid Films* **2005**, *477*, 88.
(21) Yang, C.; Jacob, J.; Mullen, K. *Macromol. Chem. Phys.* **2006**, *207*, 1107.
(22) Natori, I.; Natori, S.; Sekikawa, H.; Sato, H. *J. Polym. Sci., Part A: Polym. Chem.* **2008**, *46*, 5223.
(23) Chen, S. H.; Conger, B. M.; Mastrangelo, J. C.; Kende, A. S.; Kim, D. U. *Macromolecules* **1998**, *31*, 8051.
(24) Suda, K.; Akagi, K. *J. Polym. Sci., Part A: Polym. Chem.* **2008**, *46*, 3591.
(25) Zhou, D.; Chen, Y. W.; Chen, L.; Zhou, W. H.; He, X. H. *Macromolecules* **2009**, *42*, 1454.
(26) Chen, L.; Chen, Y. W.; Zhou, W. H.; He, X. H. *Synth. Met.* **2009**, in press.
(27) O'Neill, M.; Kelly, S. M. *Adv. Mater.* **2003**, *15*, 1135.
(28) Osaka, I.; Mccullough, R. D. *Acc. Chem. Res.* **2008**, *41*, 1202.
(29) Cianga, I.; Yagci, Y. *Prog. Polym. Sci.* **2004**, *29*, 387.
(30) Chen, L.; Chen, Y. W.; Zha, D. J.; Yang, Y. *J. Polym. Sci., Part A: Polym. Chem.* **2006**, *44*, 2499.
(31) Tang, B. Z.; Kong, X.; Wan, X.; Feng, X.-D.; Kwok, H. S. *Macromolecules* **1998**, *31*, 2419.
(32) Lam, J. W. Y.; Kong, X.; Dong, Y.; Cheuk, K. K. L.; Xu, K.; Tang, B. Z. *Macromolecules* **2000**, *33*, 5027.
(33) Grell, M.; Bradley, D. D. C.; Ungar, G.; Hill, J.; Whitehead, K. S. *Macromolecules* **1999**, *32*, 5810.
(34) Li, Y.; Vamvounis, G.; Holdcroft, S. *Macromolecules* **2002**, *35*, 6900.
(35) Lam, J. W. Y.; Tang, B. Z. *Acc. Chem. Res.* **2005**, *38*, 745.
(36) Goto, H. *Macromolecules* **2007**, *40*, 1377.
(37) Liu, J.; Yan, J.; Chen, E.; Lam, J. W. Y.; Dong, Y.; Liang, D.; Tang, B. Z. *Polymer* **2008**, *49*, 3366.